SINGLE CRYSTAL FORMATION IN CORE-SHELL CAPSULES

Marie Mettler[1], Adrien Dewandre[1], Nikolay Tumanov[2], Johan Wouters[2], Jean Septavaux[1*]

[1]: Secoya Technologies Fond des Més 4 - 1348 Louvain-la-Neuve, Belgium

[2]: Namur Institute of Structured Matter (NISM) Université de Namur, Rue de Bruxelles 61 - 5000 Namur, Belgium

Supplementary Information

Table of content

General Methods

General information

All reagents and solvents were obtained from commercial sources at reagent-purity, except the distillated water which was freshly distilled.

Poly(vinyl alcohol) (PVA, Mw 9000-10000, 80% hydrolyzed), diphenyl(2,4,6-trimethylbenzoyl) phosphine oxide (TPO, 97%), ammonium sulfate (≥99.0%), copper (II) sulfate (≥99%), glycerol (≥99.5%), glycine (≥99.0%), sodium chloride (≥99.0%), proteinase K from Tritirachium album (≥30 units/mg), Lysozyme from chicken egg white (≥40,000 units/mg) were purchased from *Sigma-Aldrich*. Ethyl acetate was purchased from *Supelco*. The polymethacrylate resin Allnex SN180232 was obtained from *Allnex*.

Production method

Production of a double emulsion

Double emulsions are formed using a Raydrop® emulsification device (*Secoya technologies srl*). The Raydrop is comprised of a metallic chamber with glass windows into which two aligned inserts are laterally disposed, each carrying a glass capillary. An injection nozzle printed using a sub-micrometer resolution 3D printer is attached to the end of the input insert. The device operates in a co-flow-focusing geometry,[1] i.e. it combines the characteristics of co-flow (cylindrical symmetry) and flow-focusing (fluid acceleration in a restriction) geometries. The injection nozzle and the outlet capillary are aligned in the chamber filled with the continuous phase under pressure. The dispersed phase is pushed into the nozzle and meets the continuous phase at the junction between the nozzle and the extraction capillary, the only outlet of the system. At this point, the pinching of the jet of the dispersed phase leaving the nozzle by the continuous phase accelerated in the extraction capillary results in the controlled formation of droplets.

Herein, the continuous phase, i.e. the external phase, was water with surfactant. Among the dispersed phases, the intermediate phase (also called shell phase) was an organic phase, and the core phase was an aqueous phase. Two reservoirs containing shell phases were prepared, one with pure organic solvent (for the priming, the stabilization of the emulsion production and the cleaning) and one with the polymethacrylate resin diluted with Ethyl Acetate. Likewise, two reservoirs containing core phases were prepared, one with water (for the priming, the stabilization of the emulsion production and the cleaning) and one with water and the solute.

The double emulsion nozzle, fed by two phases, allows the generation of double emulsions in both dripping and jetting mode. The dimensions of the nozzle used are 90 µm for the core phase, 160 µm for the shell phase and 450 µm for the extraction nozzle to form double emulsions with a mean diameter of around 250 µm.

Cross-linking of the double emulsion shell to form capsules

The shell phase is composed of polymethacrylate resin Allnex SN180232 diluted with 20 wt% Ethyl Acetate in which is added 0.1% of TPO as radical-generating photoinitiator. Once that the droplets are formed inside the Raydrop, they are carried out of the device in a straight glass outlet capillary of internal diameter 450 µm where the double emulsion is irradiated by a UV LED Curing System (*COBRA Cure FX1 FLEX*) with an intensity of 4mW/cm². Upon UV irradiation, the resin reticulates and the solid capsules with liquid core are collected at a frequency of several hundreds of capsules per second.

Peripheral instruments necessary for the operation of the microfluidic tool

The Raydrop was used in a platform which includes a camera *Ximea USB 3.1 Gen1 xiC* with an *Edmund Optics 5 X Objective* and a LED lamp to observe the double emulsion formation and *Fluigent LineUp Flow EZ 7000mbar* pressure controllers and *Fluigent Flow Unit* flowmeters (size L for the continuous phase and size M for the shell and core phases) to control the fluids.

Tubing used are PEEK or PFA tubing from *Trajan Scientific and Medical*. Every tubing diameter is adapted in order to allow working in the optimal pressure range of the pressure controllers. Inline filters porosity of 10 µm for continuous phase are used to avoid any pollution of fluids inside tubing and the Raydrop.

Production conditions of various crystals in microcapsules

The microcapsules produced contained an aqueous solution. To induce nucleation of the solute, capsules are stored in various conditions. The continuous phase and the shell phase are the same for all crystals. The continuous phase is composed of water with 2% PVA Mw 9000-10000. The shell phase is composed of Allnex SN180232 polymethacrylate resin, 20% ethyl acetate and 0,1% TPO.

Procedure for sodium chloride single crystal production:
Initial concentration of sodium chloride in the core phase was set at 200 g/L in water. The capsules were generated with flowrates of 156, 20 and 11 µL/min for the continuous, shell and core phases respectively, resulting in a mean capsule size of 299 µm. Capsules were stored in air at room temperature. Single crystals were observed after 1 day of storage.

Procedure for copper (II) sulfate single crystal production:
Initial concentration of copper (II) sulfate in the core phase was set at 200 g/L in water. The capsules were generated with flowrates of 187, 20 and 13 µL/min for the continuous, shell and core phases respectively, resulting in a mean capsule size of 277 µm. Capsules were stored in ethyl acetate at room temperature. Single crystals were observed after 2 days of storage.

Procedure for lysozyme single crystal production:
Initial concentration of lysozyme in the core phase was set at 20 mg/mL in a 5% NaCl solution at pH 5.0 (addition of NaAc 0.250M to adapt the pH). The capsules were generated with flowrates of 192, 20.1 and 17 µL/min for the continuous, shell and core phases respectively, resulting in a mean capsule size of 243 µm. Capsules were stored in a 6% NaCl solution at 4.5°C. Single crystals were observed after 3 days of storage.

Procedure for proteinase K single crystal production:
Initial concentration of proteinase K in the core phase was set at 20 mg/mL in 1.1M ammonium sulfate solution at pH 7.0 (addition of HEPES buffer pH=7 to adapt the pH). The capsules were generated with flowrates of 157, 25 and 11 µL/min for the continuous, shell and core phases respectively, resulting in a mean capsule size of 278 µm. Capsules were stored in a 1.2M ammonium sulfate solution at 4.5°C. Single crystals were observed after 2 days of storage.

Procedure for glycine single crystal production:
Initial concentration of glycine in the core phase was set at 190 g/L in water. The capsules were generated with flowrates of 177, 20 and 13 µL/min for the continuous, shell and core phases respectively, resulting in a mean capsule size of 258 µm. Capsules were stored in air at 4.5°C. Single crystals were observed after 1 day of storage.

Microscopic analysis of capsules and crystals

Microscopic analyses for the observation of capsules and crystals were performed with two microscopes: *Nikon SMZ-U Stereoscopic Zoom 1:10* and *Nikon SMZ745T*. Picture were recorded with

a *Eakins Autofocus* camera and pictures were made and recorded with the software *TopView version x64, 4.11.19728.20211022*.

Size distribution

For the size distribution determination, images recorded using a high-speed IDT XS mini 1540 camera at 1000 fps were then processed using ADM software[2]. 292 drops were measured and the diameter of each drop was averaged over 25 images.

In situ and ex situ XRD analysis of crystals

The XRD analysis can be performed through the solid shell or only on the crystal without the shell.

In situ analysis: crystals are conserved inside capsules

To make an XRD analysis on a crystal contained in a capsule, the selected capsule is mounted on a mounting loop (here a *MiTeGen Dual-Thickness MicroLoops* with 300 μm aperture). See Figure 2 in main text.

Ex situ analysis: capsules are broken and crystals are collected

It is also possible to break the capsules with a tweezer by pressing the solid shell. Once that the capsule is open, the crystal can be taken out of the shell to be placed on the sample holder for the XRD analysis.

Single-crystal X-ray diffraction

The colourless block-like single crystals of all three compound was selected and mounted on the MiTeGen MicroLoops sample holder directly in the plastic capsule. For each compound, ~4-5 capsules were tested to confirm same unit cell parameters. Single-crystal X-ray diffraction data were collected at 295 K using the Oxford Diffraction Gemini R Ultra diffractometer (Mo Kα, graphite monochromator, Ruby CCD area detector) at 295(2) K. Data collection, unit cells determination and data reduction were carried out using CrysAlis PRO software package[3]. Analytical numeric absorption correction using a multifaceted crystal model followed by empirical absorption correction using spherical harmonics. Using Olex2[4] and shelXle[5] , the structure was solved with the SHELXT 2015[6] structure solution program by Intrinsic Phasing methods and refined by full-matrix least squares on $|F|^2$ using SHELXL-2018/3[7]. Non-hydrogen atoms were refined anisotropically. Hydrogen atoms were refined independently. Final cifs and checkcif reports are provide as supplementary material, but were not submitted to CSD.

	NaCl	α-glycine	β-glycine
Chemical formula	ClNa	$C_2H_5NO_2$	$C_2H_5NO_2$
M_r	58.44	75.07	75.07
Crystal system, space group	Cubic, $Fm^{-}3m$	Monoclinic, $P2_1/n$	Monoclinic, $P2_1$
a, *b*, *c* (Å)	5.6357 (3), 5.6357 (3), 5.6357 (3)	5.1018 (9), 11.9664 (16), 5.4624 (9)	5.0947 (6), 6.2681 (5), 5.3883 (6)
α, β, γ (°)	90, 90, 90	90, 111.73 (2), 90	90, 113.232 (14), 90
V (Å^3)	179.00 (3)	309.79 (9)	158.12 (3)
Z	4	4	2
μ (mm^{-1})	1.77	0.14	0.14
Crystal size (mm)	0.15 × 0.12 × 0.06	0.15 × 0.12 × 0.08	0.25 × 0.09 × 0.07
T_{min}, T_{max}	0.833, 0.904	0.985, 0.991	0.976, 0.991

No. of measured, independent and observed [$I > 2\sigma(I)$] reflections	212, 26, 26	5261, 1058, 806	1996, 1053, 921
R_{int}	0.023	0.040	0.022
$(\sin\theta/\lambda)_{max}$ ($Å^{-1}$)	0.710	0.761	0.761
$R[F^2 > 2\sigma(F^2)]$, $wR(F^2)$, S	0.010, 0.024, 1.25	0.045, 0.131, 1.10	0.043, 0.097, 1.07
No. of reflections	26	1058	1053
No. of parameters	4	66	66
No. of restraints	0	0	1
$\Delta\rho_{max}$, $\Delta\rho_{min}$ ($e \cdot Å^{-3}$)	0.11, -0.09	0.28, -0.32	0.26, -0.24

Supplementary figures

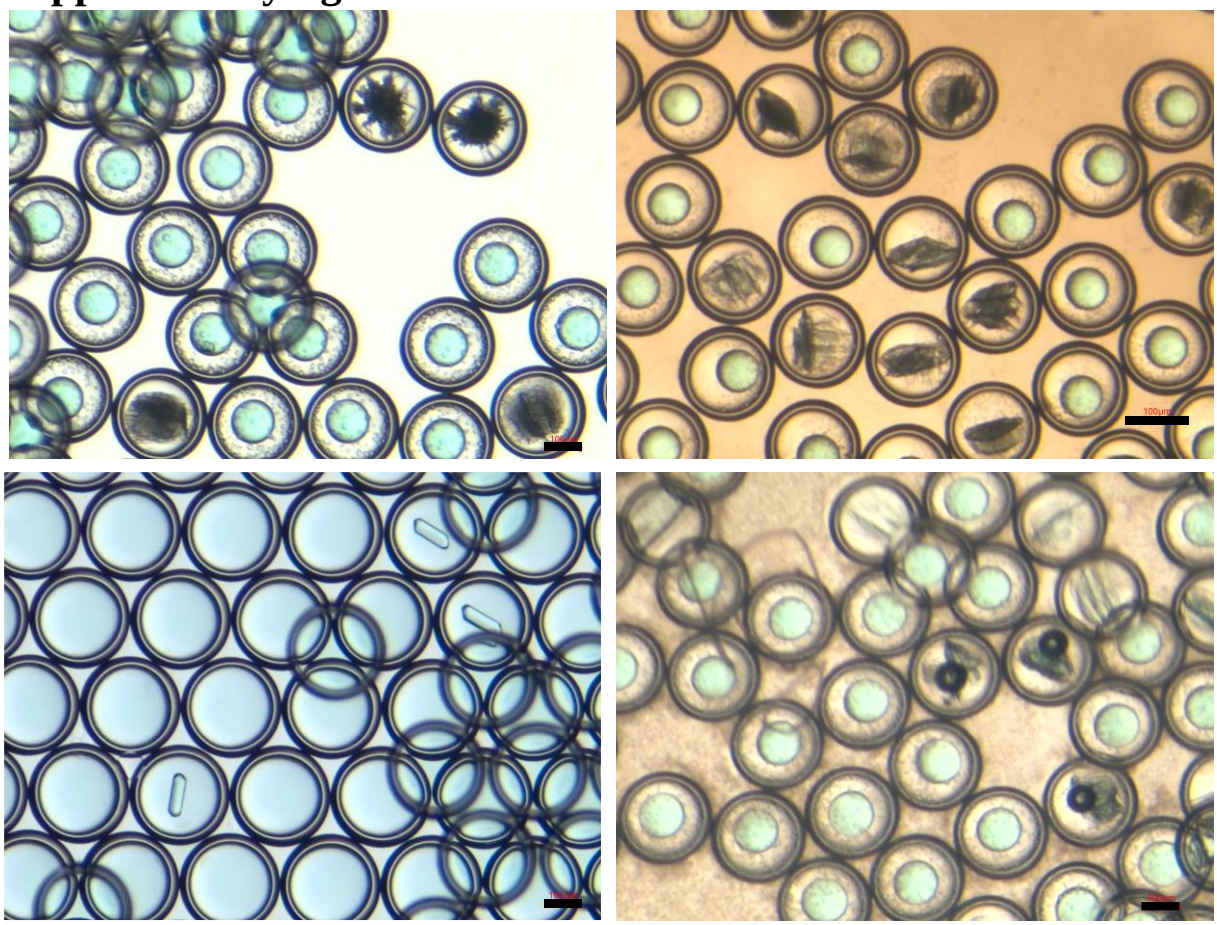

Figure S1: Samples of capsules containing 200 g/L $CuSO_4$ in water after 48 hours of storage at room temperature in top left: ethanol, top right: acetone, bottom left: ethyl acetate, bottom right: 2-propanol. Scale bar are 100 µm.

Sample	Q(continuous)	Q(shell)	Q(core)	ED	ID	Shell thickness
	µL/min	µL/min	µL/min	µm	µm	µm
1	163	27	17	312	258	54
2	162	21	17	315	274	41
3	157	17	17	320	286	34
4	158	12	17	326	264	31
5	158	7	17	334	309	25

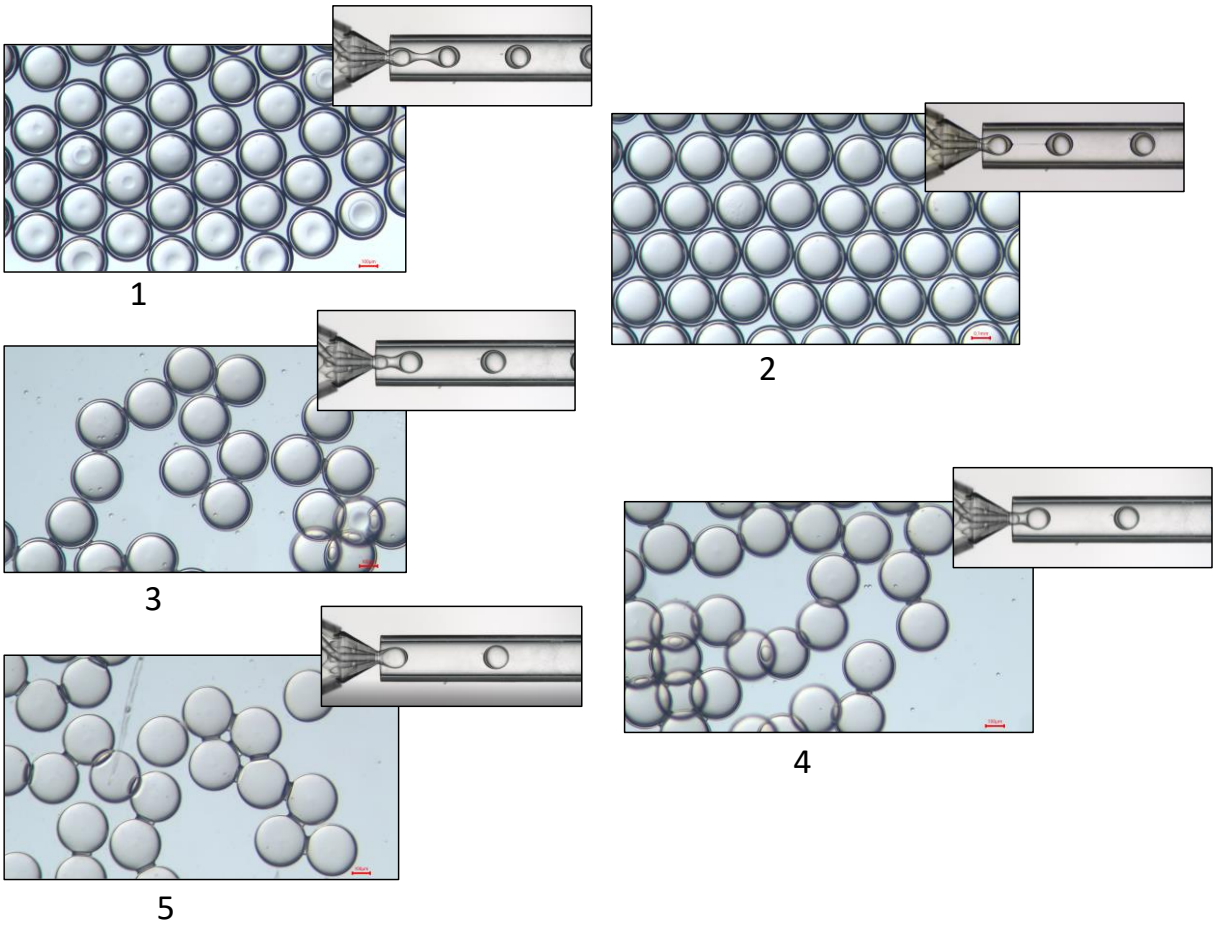

Figure S2: Pictures of capsules with shell thicknesses ranging from 25 to 54 µm, with the associated generation conditions. Windows picture the emulsion phase for each condition.

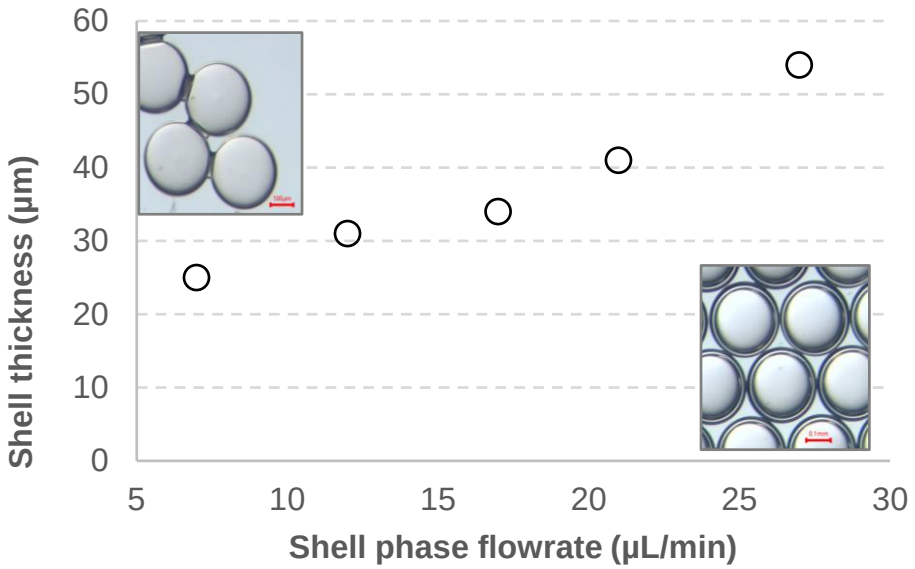

Figure S3 Evolution of the shell thickness of capsules as a function of the shell phase flowrate during the double emulsion generation step. Core and continuous phase flowrates were set at 17 and 160 µL/min respectively. Top left picture displays capsules with a 25 µm shell; bottom right picture shows 54 µm thick capsules.

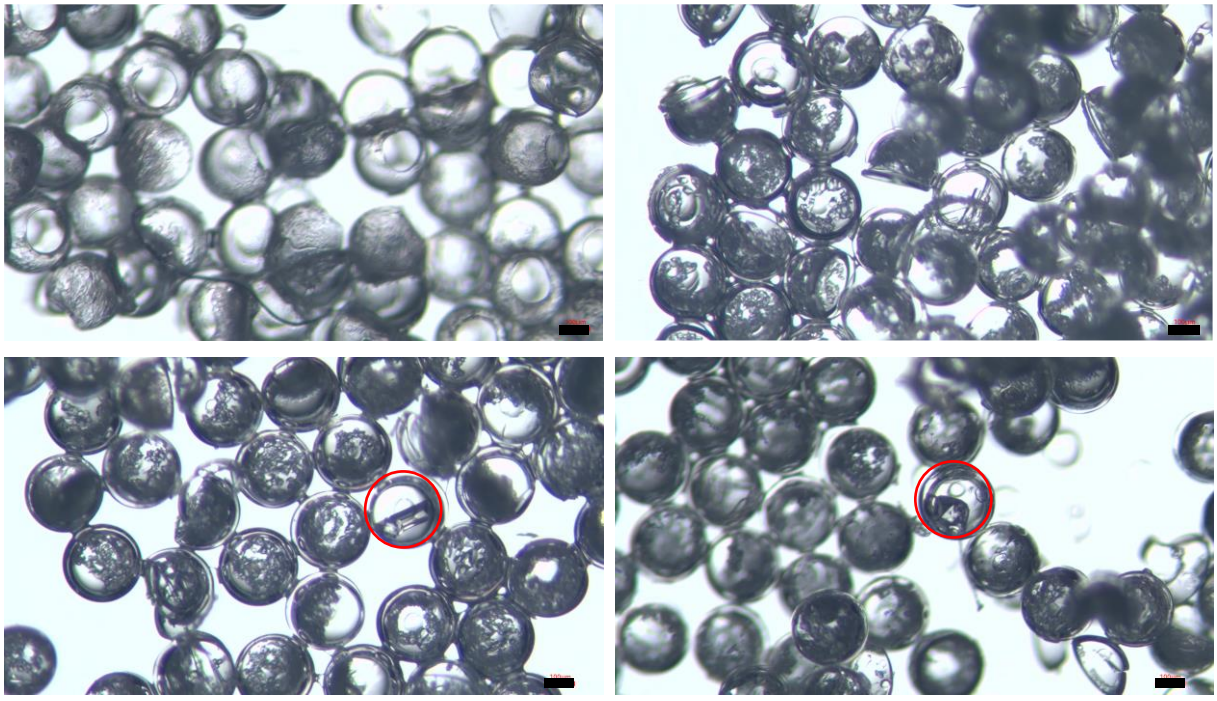

Figure S4: Pictures of capsules containing 190 g/L of glycine in water after 48 hours of storage at 4.5°C (at air) with a shell thickness of top left: 25 µm, top right 41 µm, bottom left 45 µm, bottom right 49 µm. Circled capsules contained only one crystal. Scale bars are 100 µm.

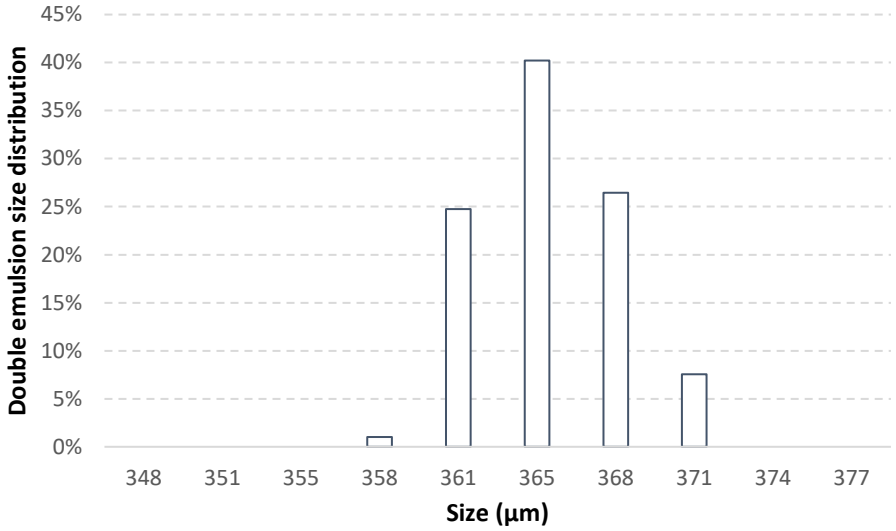

Figure S5: Typical double emulsion size distribution, generated with core, shell and continuous phase flowrates of 30, 45 and 500 µL/min respectively. Pixel size 11.6 µm, 5x zoom and 0.7x diffuser offers a 3.3 µm resolution. Coefficient of variation calculated as 0.8%.

1 A. Dewandre, J. Rivero-Rodriguez, Y. Vitry, B. Sobac and B. Scheid, *Sci Rep*, 2020, **10**, 21616.

2 Z. Z. Chong, S. B. Tor, A. M. Gañán-Calvo, Z. J. Chong, N. H. Loh, N.-T. Nguyen and S. H. Tan, *Microfluid Nanofluid*, 2016, **20**, 66.

3 Rigaku Oxford Diffraction, 2020.

4 O. V. Dolomanov, L. J. Bourhis, R. J. Gildea, J. a. K. Howard and H. Puschmann, *Journal of Applied Crystallography*, 2009, **42**, 339–341.

5 C. B. Hübschle, G. M. Sheldrick and B. Dittrich, *Journal of applied crystallography*, 2011, **44**, 1281–1284.

6 G. M. Sheldrick, *Acta Crystallographica Section A Foundations and Advances*, 2015, **71**, 3–8.

7 G. M. Sheldrick, *Acta Crystallographica Section C Structural Chemistry*, 2015, **71**, 3–8.